Intelligent Coordination of Traditional Power Plants and Inverters Air Conditioners Controlled With Feedback-Corrected MPC in LFC

Oshnoei, Arman; Khezri, Rahmat; Oshnoei, Soroush; Mahmoudi, Amin; Azzouz, Maher A.; Awad, Ahmed S.A.

Published in:
IEEE Transactions on Circuits and Systems I: Regular Papers

DOI (link to publication from Publisher):
10.1109/TCSI.2023.3330323

Publication date:
2024

Document Version
Publisher's PDF, also known as Version of record

Intelligent Coordination of Traditional Power Plants and Inverters Air Conditioners Controlled With Feedback-Corrected MPC in LFC

Arman Oshnoei, *Member, IEEE*, Morteza Kheradmandi, *Member, IEEE*, Rahmat Khezri, *Senior Member, IEEE*, Soroush Oshnoei, *Associate Member, IEEE*, Amin Mahmoudi, *Senior Member, IEEE*, Maher A. Azzouz, *Senior Member, IEEE*, and Ahmed S. A. Awad, *Senior Member, IEEE*

***Abstract*— Demand response programs have been receiving more serious attention as alternatives for participating in load frequency control. Inverter air conditioners (IAC) are acknowledged as suitable devices for demand response due to their increasing contribution to network consumption. Despite their potential, their use presents challenges, including delayed responses, variable interference, and the absence of coordination with traditional generation units, which may affect control performance. Also, existing control strategies fail to consider operational and physical constraints, resulting in possible model mismatches. In this paper, a model predictive control with feedback correction (MPCFC) is proposed to dispatch control signals to the IACs so they can effectively participate in the frequency control of an interconnected power system. The feedback correction method is presented to enhance prediction accuracy in the MPC and weaken the influence of model parameter mismatches and external disturbances. Furthermore, to minimize the impacts of communication delays on frequency overshoot/undershoot, this study introduces an intelligent supervisory coordinator based on an artificial neural network to coordinate the reaction of traditional generation units and IACs to correct significant frequency variations brought on by the time delays. The effectiveness of the developed control scheme is verified through numerical studies by comparing it with the IAC with PI and MPC controllers (without coordinator) and the system without IACs. Case studies are investigated on a two-area power system in MATLAB/Simulink environment, and the OPAL-RT real-time simulator is used to validate the results.**

Manuscript received 6 May 2023; revised 9 August 2023 and 26 September 2023; accepted 17 October 2023. This article was recommended by Associate Editor Y. Tang. *(Corresponding author: Arman Oshnoei.)*

Arman Oshnoei is with the Department of Energy, Aalborg University, 9220 Aalborg, Denmark (e-mail: aros@energy.aau.dk).

Morteza Kheradmandi is with Institut National Polytechnique de Grenoble, 38058 Grenoble, France (e-mail: kheradmandi@gmail.com).

Rahmat Khezri and Amin Mahmoudi are with the College of Science and Engineering, Flinders University, Adelaide, SA 5042, Australia (e-mail: rahmat.khezri2@gmail.com; amaminmahmoudi@gmail.com).

Soroush Oshnoei is with the Department of Electrical and Computer Engineering, Aarhus University, 8000 Aarhus, Denmark (e-mail: soroush_oshnoei@yahoo.com).

Maher A. Azzouz is with the Electrical Engineering Department, Qatar University, Qatar (e-mail: mazzouz@qu.edu.qa).

Ahmed S. A. Awad is with the Department of Electrical and Computer Engineering, Sultan Qaboos University, Muscat 123, Oman (e-mail: a.awad1@squ.edu.om).

Color versions of one or more figures in this article are available at https://doi.org/10.1109/TCSI.2023.3330323.

Digital Object Identifier 10.1109/TCSI.2023.3330323

***Index Terms*— Feedback correction, inverter air conditioner, artificial neural networks, load frequency control, model predictive control, multi-area power systems.**

NOMENCLATURE

Acronyms

AC	Air conditioner.
ACE	Area control error.
AGC	Automatic generation control.
AMD	Absolute maximum deviation.
ANN	Artificial neural network.
CGU	Conventional generation unit.
DR	Demand response.
ESS	Energy storage system.
GRC	Generation rate constraint.
IAC	Inverter air conditioner.
ITSE	Integral of time multiplied by the squared error.
LFC	Load frequency control.
PFC	Primary frequency control.
SFC	Secondary frequency control.
MPC	Model predictive control.
MPCFC	Model predictive control with feedback correction.
PI	Proportional integral.
PMU	Phasor measurement unit.
RMS	Root mean square.
ROCOF	Rate of change of frequency.
SCA	Sine cosine algorithm.
WAMS	Wide area monitoring system.

Parameters

a, b	Proportional and integral gains of PI.
c_p, c_q	IAC's constant coefficients.
$f_{IAC}^{\max}, f_{IAC}^{\min}$	IAC's operating frequency limit allowed values.
i, j	Indices for control areas.
m	Number of control areas.
C_r	Room thermal mass.
D	Load damping constant.

E_{tc}	Equivalent thermal conductance between the outdoor and room environments.
M	Equivalent inertia constant.
P_{IAC}	IAC's operating power.
Q_{IAC}	IAC's refrigerating capacity.
Q_r	Room heat gain.
T_f, T_p	Integrating time length for frequency deviation and tie-line power.
T_{ij}	Synchronizing torque coefficient between areas i and j.
V_r	Room volume.
α, ψ	MPC's input/output weighting coefficients.
β	Frequency bias coefficient.
δ_{CGU}, δ_{IAC}	Distribution coefficients of ACE signal to the CGU and IAC aggregator.
ρ_d	Air density.
θ_o	Outdoor temperature.
θ_r	Room temperature.
θ_{st}	IAC's Set temperature.

Variables

f_{IAC}	IAC's operating frequency.
$K_{i,s}$, $K_{p,s}$	Supplementary integral and proportional gains by ANN.
S_i, S_p	Scaling coefficients for proportional and integral gains in ANN.
Δf	Frequency deviation.
ΔP_{gas}, ΔP_{hyd}, ΔP_{th}, ΔP_{IAC}, ΔP_{tie}	Power deviation in gas, hydro and thermal units and in IAC and tie-line power.
ΔP_L	Load power variation.
V_{IAC}	MPC control signal to IACs.

I. Introduction

A. Background and Motivation

THE mismatch between generation and consumption needs to be corrected immediately in cases where load values change suddenly to avoid severe frequency violations. With their governor and AGC loops, CGUs are used traditionally as the prime candidates for the LFC [1], [2]. The CGUs, however, raise various issues due to the slow dynamics of the mechanical parts, air pollution problems, and high operation and reserve costs [3], [4].

The DR programs have recently drawn attentions thanks to the substantial progresses in communication and information technologies, which have enabled the consumption side to contribute to the LFC problems [5], [6]. The appliances can participate in the LFC within a DR program by switching between the on/off status or by varying the consumption in response to frequency variations. Air conditioners, heat pump water heaters, refrigerators, and plug-in electric vehicles are suitable DR options for participating in the LFC. ACs have generated a lot of interest because they are easily controlled and have no impact on consumer comfort [7]. The ACs fall into two categories of fixed speed and inverter-based ACs. While the consumption of fixed-speed ACs can only be controlled by switching between on/off modes of the compressor, the power consumption in IACs can be continuously controlled through modifying the compressor's working frequency [8]. In power systems, aggregated form of IACs, if they receive appropriate LFC signals, can contribute to frequency regulation [9]. Compared to individual IACs, the aggregation enables the attainment of virtually higher powers. Furthermore, the system operator can consider the IAC aggregator as a single entity, facilitating the control process.

Signal transmission from the control center to aggregators and then to the individual IACs requires a large communication system infrastructure. WAMS has facilitated signal transmission from remote sites so that power systems have achieved efficient wide-area control. Using WAMS, however, poses a time delay challenge in the measurement and dispatch of control signals via communication channels [10]. The frequency control of power systems involving DR programs is impacted by lengthy time delays [11]. As a result, it appears crucial to establish IAC and CGU cooperation, which is unique to this paper. Furthermore, power generation and consumption characteristics smart grids require a frequency controller that combines robust performance with rapid responsiveness. Therefore, a frequency controller for IACs is needed to minimize the effects of diverse power imbalances.

B. Literature Review

Regarding IAC participation in the frequency regulation markets, some research have been done. In [12], IACs are supported by a comparable model that modifies their set points in order to keep system frequency. In [13] and [14], IACs are utilized to offer PFC services, while [15] proposes a coordinated control approach for IAC units to participate in SFC, improving regulatory service by increasing frequency reserve. In [8], IACs can be controlled as generators to allow frequency control and are comparable to a traditional unit. In [16], the authors propose the allocation strategy of regulating capacity to plan aggregated IACs in various time scales. In summary, current research mostly focuses on the dispatch and modeling techniques for IACs, while the design of reliable controllers to generate effective control signals for an efficient contribution of IACs to the SFC has received scant attention. Studies on control strategies for IACs in secondary frequency control are limited to [16] and [17]. In [16], a proportional control method is proposed for IACs in LFC. In [17], a PI-based approach is employed to deal with the control actions for the IACs to respond to the regulation signals. The operational and physical constraints have received little attention in these studies.

MPC is recognized as a modern control method for power system control problems. The MPC is designed based on an equivalent state-space model of the system. An optimization procedure is conducted at each time interval while satisfying a set of system constraints. The MPC is successfully applied in the LFC problems as an effective alternative to classic controllers [18], [19], [20]. In [21], the IACs are controlled using an MPC in the LFC problem. Although this study prioritizes the development of prediction models, cost

functions, and computational efficiency to achieve satisfactory performance, it overlooked the impact of model mismatches. In other words, if the model is inaccurate, it may lead to poor control performance. Hence, a model error compensation method is required in the MPC structure to compensate for prediction error, which is addressed in this paper.

C. Research Gap

In summary, a gap has been identified from past studies as below:

1) Potential technical challenges might arise due to delayed responses or variable interference of the IACs. It is vital to establish a coordination mechanism between the IAC and CGU units to tackle these emerging issues.
2) Although some control strategies for IACs in secondary frequency control have been proposed, these methods often overlook the crucial aspects of operational and physical constraints. This omission can lead to potential model mismatches and affect control performance.
3) There is a research gap in addressing the need for model error compensation within the MPC structure. Such compensation is essential to account for prediction errors and ensure the robustness of the control system, especially when dealing with the complexities and uncertainties inherent in the system.

D. Contributions

To bridge the mentioned gaps, this paper presents an MPCFC for controlling the IACs via aggregators for efficient contribution in the SFC of a multi-area power system with wind energy and CGUs. The feedback correction strategy is constructed to improve prediction accuracy and create disturbance rejection ability in the MPC structure. The scaling factors of the MPCFC are optimized using a sine cosine algorithm. To overcome the time delay effects in the considered system with IACs, an artificial neural network-based coordinator between the secondary frequency control of CGUs and IACs to cover the time delays of demand response is developed. The proposed coordinator delivers ancillary parameters for the PI controller integrated into the CGUs' control loop based on data from the ACE and IACs regarding the measured power. The main contributions of this paper can be itemized as follows:

1) Proposing an MPCFC to dispatch control signals to the IACs efficiently. This approach enhances the prediction accuracy in the MPC, which minimizes the effects of model parameter mismatches and external disturbances.
2) Introducing an intelligent supervisory coordinator designed based on ANN. This coordinator synchronizes the reactions of traditional generation units and IACs to mitigate frequency deviations caused by communication delays, hence optimizing the frequency control performance of the interconnected power system.
3) Conducting a comprehensive effectiveness analysis of the proposed controller, comparing it with the IAC aggregators equipped with MPC, LQR, Fuzzy-PI, and the system without IACs.
4) Executing case studies on a two-area power system in the MATLAB/Simulink environment and utilizing the OPAL-RT real-time simulator for result validation.

E. Paper Organization

The remainder of this paper is organized as follows. Section II explains the equivalent model of IACs to participate in the LFC. The model predictive control design is developed in Section III. The coordination of IAC aggregators and CGUs based on artificial neural network is presented in Section IV. Section V explains the case study, including the power system under the study and the simulation results. Finally, Section VI concludes the paper.

II. Proposed Frequency Control Scheme

A. System Structure

Transmission lines, known as tie-lines, connect multiple areas in large-scale power systems. A schematic view of an area consisting of CGUs, aggregated IACs, and renewable energy resources is displayed in Fig. 1.

The IAC control, as the figure illustrates, comprises central and local control centers, a communication network, and aggregated IACs. The information exchange between the central control center and local control center and between local control center and IACs are bidirectional. These connections are feasible under the smart grid concept, which utilizes communication and information technology. The local centers may deal with IACs of different sizes and characteristics. These centers announce the measured and the available power of IACs to the main control center. The PMUs in the areas where an LFC scheme is to be implemented measure the tie-line power and frequency signals. These signals are also sent to the main control center through communication links. The main control center then calculates and sends portions of an ACE signal to the local control centers based on the announced available IACs.

B. Proposed LFC Scheme

The frequency deviation in area i can be written in the time domain as

$$\frac{\mathrm{d}\Delta f_i}{\mathrm{d}t} = -\frac{D}{M}\Delta f_i + \frac{1}{M}\left(\Delta P_{th_i} + \Delta P_{gas_i} + \Delta P_{hyd_i} - \Delta P_{tie_i} - \Delta P_{IAC_i} - \Delta P_{L_i}\right) \quad (1)$$

where the variation in the total power leaving area i can be written as follows:

$$\Delta P_{tie_i} = 2\pi\left(\sum_{\substack{j=1\\ j\neq i}}^{m} T_{ij}\right)\Delta f_i - 2\pi\sum_{\substack{j=1\\ j\neq i}}^{m}\left(T_{ij}\Delta f_j\right). \quad (2)$$

As (1) implies, the CGUs include thermal, hydro, and gas units. An equivalent model that is derived from the thermal and electrical models is required to evaluate the deviation in the power of IAC aggregators in terms of the frequency deviation. The thermal model is formulated as follows [16]:

$$C_r V_r \rho_d \frac{\mathrm{d}\Delta\theta_r(t)}{\mathrm{d}t} = \Delta Q_r(t) - \Delta Q_{IAC}(t) \quad (3)$$

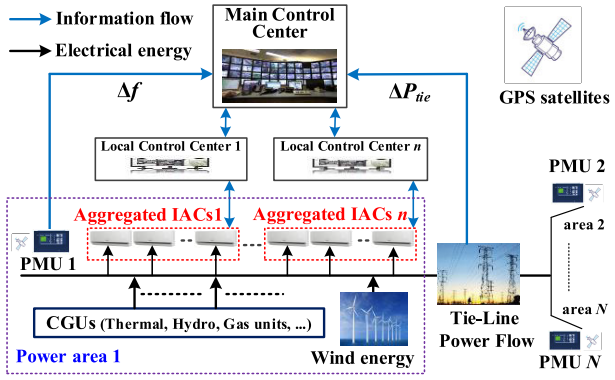

Fig. 1. The framework of the SFC service in the presence of IAC aggregators.

where the variation in room heat gain can be expressed proportional to the variation in the indoor temperature as follows:

$$\Delta Q_r(t) = E_{tc}\Delta\theta_r(t). \tag{4}$$

where E_{tc} is equivalent thermal conductance between the room air and outdoor. The variation in the IAC operating power and in the IAC refrigerating capacity is described in terms of the IAC frequency deviation as below:

$$P_{IAC}(t) = p(t)f_{IAC}(t) + c_{p2} \tag{5}$$

$$Q_{IAC}(t) = q(t)f_{IAC}(t) + c_{q2} \tag{6}$$

where

$$p(t) = \frac{c_{p1}}{T_c}e^{\frac{-1}{T_c}t}; \quad q(t) = \frac{c_{q1}}{T_c}e^{\frac{-1}{T_c}t} \tag{7}$$

where c_{p1}, c_{p2}, c_{q1}, and c_{q2} are IAC constant coefficients; and T_c is the time constant of the compressor.

The IAC working frequency is controlled by controlling compressor speed and should remain within a defined range between $f_{IAC}^{\max}$ and $f_{IAC}^{\min}$. During regular operation, without engaging in frequency regulation, a classic PI controller is used to control the IAC operating frequency by using the difference between θ_r and θ_{st} as follows:

$$\Delta f_{IAC}(t) = K_a\Delta\theta_{dev}(t) + K_b\int\Delta\theta_{dev}(t)\mathrm{d}t \tag{8}$$

where

$$\Delta\theta_{dev}(t) = \Delta\theta_r(t) - \Delta\theta_{st}(t). \tag{9}$$

In participating in frequency control, however, the IAC operating power should be associated to vary according to system frequency deviation. For this aim, the local control centers are provided with regulation signals V_{IAC} so as to regulate the output power of the aggregated IACs. are created by observing the frequency deviations in control areas. The IAC frequency deviation in (8) is rewritten as follows:

$$\Delta f_{IAC}(t) = V_{IAC}(t) + K_a\Delta\theta_{dev}(t) + K_b\int\Delta\theta_{dev}(t)\mathrm{d}t. \tag{10}$$

This equation accommodates the IAC thermal and electrical models. Given the fact that in the load frequency control, the IAC set doesn't change over such a brief time. The following is how the IAC's operational power changes in response to the power system's regulatory signal:

$$\Delta P_{IAC}(t) = c_p\left(V_{IAC}(t) + K_a\Delta\theta_r(t) + K_b\int\Delta\theta_r(t)\mathrm{d}t\right). \tag{11}$$

It is clear from (11) that the regulation signal V_{IAC} can be used to change the IAC operational power for efficient frequency control. From equation (1) to (11), the IAC's operational power variation can be shown in the frequency domain as below:

$$\Delta P_{IAC}(s) = \frac{c_{p1}(T_A s + 1)}{(T_A s + 1)(T_c s + 1) + \eta L(s)}V_{IAC}(s) \tag{12}$$

where

$$T_A = \frac{C_r V_r \rho_d}{E_{tc}}; \quad \eta = \frac{c_{q1}}{E_{tc}} \tag{13}$$

$L(s)$ is the IAC's internal temperature controller adjusts the operating frequency to maintain the indoor temperature at its setpoint and can be designed using a PI controller as shown by:

$$L(s) = K_a + \frac{K_b}{s} \tag{14}$$

where K_a and K_b represents the gains of PI controller.

III. Model Predictive Control With Feedback Correction

A. Overall Description

MPC is an optimal closed-loop control methodology based on system model within a finite time horizon [22]. The proposed MPC of this paper consists of three parts: rolling optimization, prediction model, and feedback correction [23]. The MPC is a viable option for controlling complex systems as it incorporates an optimization technique and can deal with restrictions via a finite time horizon. In a sampling period of T_s, the controller computes future control signals by optimizing an objective function that comprises the model and present and previous signals of the system [24].

In this paper, the MPC is designed to give the control signals to aggregated IACs to participate in frequency regulation. The objective function is optimized while taking into account some restrictions. These restrictions include device restrictions such as the output power of IACs and system restrictions such as the ACE change signal.

B. Prediction Model and Feedback Correction

The weighted frequency deviation and the change in tie-line power, as indicated in (15), are summed to determine the ACE [25]:

$$ACE_i = \Delta P_{tie_i} + \beta_i\Delta f_i. \tag{15}$$

The IAC aggregator and CGU are supplied with fractions of the ACE as below:

$$ACE_{IAC_i} = \delta_{IAC}ACE_i \tag{16}$$

$$ACE_{CGU_i} = \delta_{CGU}ACE_i. \tag{17}$$

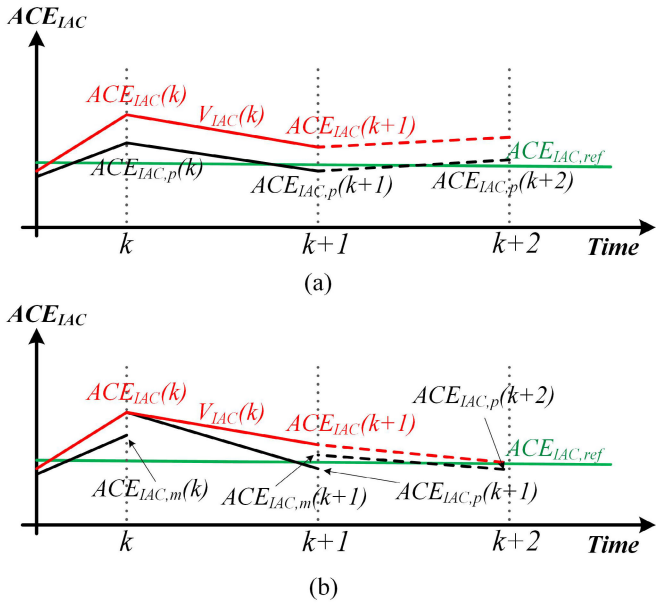

Fig. 2. Operation process of (a) MPC, (b) MPCFC.

The distribution coefficients δ_{IAC} and δ_{CGU} add up to unity. The IACs participate in frequency regulation service based on the provided ACE_{IAC}. Each IAC only responds to the signal if its value is outside a specified range. In essence, no IAC will participate in LFC if ACE_{IAC} falls within this range. The IACs are designed to adjust power consumption based on ACE_{IAC} values, but only if the room temperature for each IAC remains within the maximum allowable deviation. The variation in frequency and tie-line power given in (1) and (2) can be discretized by utilizing the first-order Euler technique as in (18) and (19), shown at the bottom of the next page, respectively. Then, the predicted value of $ACE_{IAC_i,p}$ is computed by the prediction model as

$$ACE_{IAC_i,p}(k+1|k) = \Delta P_{tie_i}(k+1|k) + \beta_i \Delta f_i(k+1|k). \quad (20)$$

The operation process of the conventional MPC scheme with disturbances (stochastic wind energy and load) is depicted in Fig. 2(a). This figure is a conceptual guide to the operational sequence and interactions within the MPC controller. At instant k, due to the presence of disturbances, the predicted value $ACE_{IAC}, p(k)$ is not identical to the measured value $ACE_{IAC}(k)$, thus the optimal control command $V_{IAC}(k)$ works on the system in the state of $ACE_{IAC}(k)$ and optimization computation of $V_{IAC}(k+1)$ performs as well. The black dashed line is then emanated from state $ACE_{IAC}, p(k+1)$. At instant $k+1$, measured value $ACE_{IAC}(k+1)$ is accessible, the predicted value $ACE_{IAC}, p(k+2)$ is calculated. The Black dashed line will be translated parallel from point $ACE_{IAC}, p(k+1)$ to $ACE_{IAC}(k+1)$, then the red dashed line arises in Fig. 2(a). As shown in Fig. 2(a), the predicted value $ACE_{IAC}, p(k+1)$ is not at the expected point and is distant from the reference point. This implies that the specified control command may not be optimal when it operates with model mismatches. A feedback correction is introduced in the control loop to enhance the accuracy of the prediction. This method adjusts the prediction model output at the current instant by prediction error at the last instant, and eventually, the output of the prediction model is corrected. For this goal, the ACE signal is modified by subtracting a fraction of the signal growth obtained in the precedent step as follows:

$$ACE_{IAC_i,m}(k+1|k) = ACE_{IAC_i,p}(k+1|k) + p_i(k) \quad (21)$$

where $p_i(k)$ is calculated as:

$$p_i(k) = \gamma_i \left(ACE_{IAC_i,p}(k) - ACE_{IAC_i,p}(k+1|k) \right). \quad (22)$$

The prediction accuracy is closely associated with the correction coefficient. A too small or too large correction coefficient can affect the predicted error ACE_{IAC_i}. The principle of the MPCFC strategy is illustrated in Fig. 2(b). As can be seen, in comparison to Fig. 2(a), the modified prediction value $ACE_{IAC_i,m}(k+1)$ is more in line with the measured value, which means that optimal control performance is retained based on the control command computed by $ACE_{IAC_i,m}$(k+1).

C. Rolling Optimization

The MPC is supplied with the modified error value ACE_{IAC,m_i}. In order to bring the system output as closely as feasible to a reference output $ACE*_{IAC_i}$ with the least amount of control effort, the MPC then sends the system model a control signal, V_{IAC_i}. It is assumed that the reference value is zero. The control signal is generated in order to attain the following objective function's optimal value:

$$\min Q_{MPC} \left(ACE_{IAC,m_i}(k+1|k) - ACE^*_{IAC_i} \right)^2 + R_{MPC} V^2_{IAC_i}. \quad (23)$$

The optimization problem is constrained by the following limits:

$$ACE^{min}_{IAC_i} \le ACE_{IAC_i}(k) \le ACE^{max}_{IAC_i} \quad (24)$$

$$V^{min}_{IAC_i} \le V_{IAC_i}(k) \le V^{max}_{IAC_i}. \quad (25)$$

The optimization process is repeated at sample $k+1$ by using the key data at sample k. The overall MPC control scheme for the IAC aggregator is shown in Fig. 3. The weighting coefficients Q_{MPC} and R_{MPC} in the above equation are tuned through optimizing the following objective function:

$$\min \sum_{i \in \psi} \int_0^{T_f} t \Delta f_i^2(t) \mathrm{d}t + \sum_{\substack{i,j \in \psi \\ i \neq j}} \int_0^{T_p} t \Delta P^2_{tie_{ij}}(t) \mathrm{d}t. \quad (26)$$

As (26) implies, the objective function is a summation of the integral of time multiplied by the squared error over the areas. An SCA is employed to solve the optimization problem [26]. The optimization is constrained by the following limits:

$$Q^{\min}_{MPC} \le Q_{MPC} \le Q^{\max}_{MPC} \quad (27)$$

$$R^{\min}_{MPC} \le R_{MPC} \le R^{\max}_{MPC} \quad (28)$$

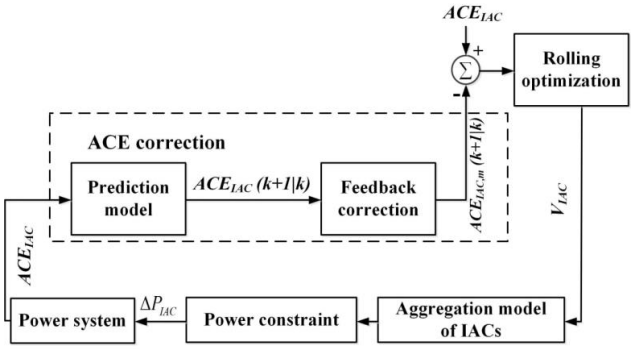

Fig. 3. Block diagram of the proposed MPCFC for the IAC aggregators.

IV. Supervisory Coordinator Design by Artificial Neural Network

Making use of the demand response programs for load-frequency control implicates unavoidable time delays in propagation links. When there is a disturbance, like a change in the load, the CGUs start to restore the power balance by raising or lowering the generation. If the IACs as supplementary controls receive the command and respond with a lengthy delay, the power surplus or deficit caused by power injection/withdrawal of IACs may lead to significant frequency overshoots/undershoots, and may lead to system instability. It is assumed that ACE_{IAC_i} is sampled and sent at instances $t_r^a, r = 1, 2, \ldots, k$ to build the ACE sequence $\widehat{ACE}_{IAC_i}(t_r^a)$. The IAC controller receives the signal samples with time delays τ_r at instances $t_r^b, r = 1, 2, \ldots, k$.

It is assumed that the signal is conveyed with a time delay, and whose magnitude remains unchanged. Mathematically stated,

$$ACE_{IAC_i}(t_r^b = t_r^a + \tau_r) = \widehat{ACE}_{IAC_i}(t_r^a). \tag{29}$$

The IAC aggregator responds to signal value ACE_{IAC_i} supplied at $t = t_r^b$, which is equal to that at an earlier time $t = t_r^a$, whereas the actual $\widehat{ACE}(t = t_b)$ may differ. The communication delay process is linearized using the Padé approximation [27]. The Padé function is written as follows:

$$ACE'_{IAC_i}(s) = e^{\tau_r s} ACE_{IAC_i}(s) \approx J_{pq}(s) ACE_{IAC_i}(s) \tag{30}$$

where

$$J_{pq}(s) = \frac{\sum_{k=0}^{p} \frac{(p+q-k)!p!}{(p+q)!k!(p-k)!}(-\tau_r s)^k}{\sum_{k=0}^{q} \frac{(p+q-k)!q!}{(p+q)!k!(q-k)!}(-\tau_r s)^k} \tag{31}$$

where p and q stand for the Padé approximation function's numerator and denominator. The numerator and denominator polynomials in this research are third-order approximates.

An ANN supervisory coordinator is presented to deal with the time delay and the ensuing frequency overshoots/undershoots caused by the in-coordination between the delayed demand response and generation units. Thus, not only the ANN serves to deal with the control task but also to coordinate the CGUs and the IACs. The ANN coordinator is in charge of minimizing the frequency and tie-line power deviations in case of rapid power changes in the power system. Intelligent controllers can be used as supervisory coordinators to enhance the performance of classic controllers in complex nonlinear power system models with uncertainties [28]. Neural network is among the most popular intelligent supervisory coordinators and is successfully applied for online adjusting of PI controller coefficients. An ANN supervisory coordinator is used in this paper for online and fine-tuning of the PI controllers in the control loop of generators. This intelligent coordination methodology provides a smooth performance in transients. In developing the ANN coordinator, the deviation of the output power of the aggregated IACs as well as the ACE signal are used as inputs to cover the effects of time delay and uncertainties. Fig. 4 shows how the ANN supervisory coordinator is used in the proposed LFC scheme.

The designed ANN comprises an input and an output layer together with two hidden layers. As the key element of ANN, each neuron has three parameters: neuron weights ω_u, a bias value φ, and an activation function $g(net)$. If the input data is labeled by χ_u, then, the output of the layer is then calculated by:

$$y_m = g\left(\sum_{u=1}^{n} w_u \chi_u + \varphi\right) j = 1, 2, \ldots, L \tag{32}$$

While different functions (e.g., sign, logsigmoid, and tan-sigmoid) can be used for the activation function, a sign model is used herein [28]. The considered ANN is trained by the response for a set of different load disturbance scenarios and based on the power system model described in Fig. 4. The learning process aims to minimize the mean squared error, defined as:

$$E = \frac{1}{2}\sum_{r=1}^{N}\left(ACE - ACE_{ref}\right)^2 \tag{33}$$

where N is the total number of samples; and ACE_{ref} denotes the reference ACE signal, which is set to zero. The input layer of the ANN contains ten linear neurons. The hidden layers contain twenty nonlinear neurons. The nonlinear functions in the hidden layers can provide a smooth update of the neural network weights throughout the procedure. The output layer of ANN contains two linear neurons corresponding to the control

$$\Delta f_i(k+1|k) = \left(1 - \frac{DT_s}{M}\right)\Delta f_i(k) + \frac{T_s}{M}\left(\Delta P_{th_i}(k) + \Delta P_{gas_i}(k) + \Delta P_{hyd_i}(k) - \Delta P_{tie_i}(k) - \Delta P_{IAC_i}(k) - \Delta P_{L_i}(k)\right). \tag{18}$$

$$\Delta P_{tie_i}(k+1|k) = 2\pi T_s\left(\sum_{\substack{j=1 \\ j\neq i}}^{m} T_{ij}\right)\Delta f_i(k) - 2\pi\sum_{\substack{j=1 \\ j\neq i}}^{m}\left(T_{ij}\Delta f_j(k)\right) + \Delta P_{tie_i}(k). \tag{19}$$

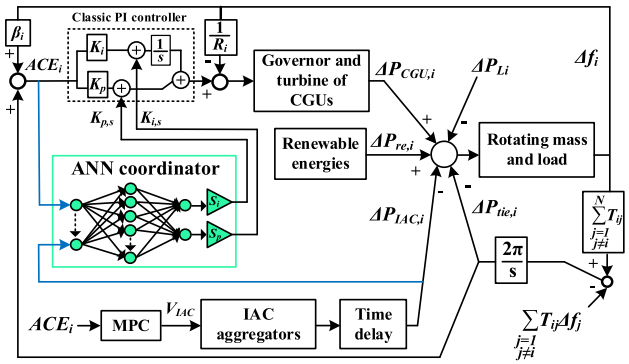

Fig. 4. System frequency response model incorporating an IAC and ANN supervisory coordinator.

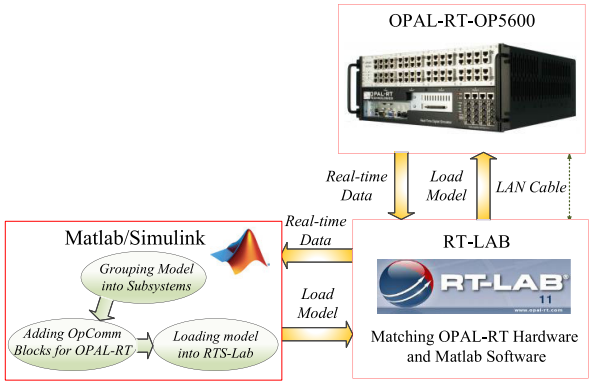

Fig. 5. Real time experimental setup.

variables, namely the proportional and integral gains of the PI controller. The back-propagation supervised learning approach is used for the feedback process [29].

In this study, it is assumed that the parameters of the PI controllers (i.e., proportional and integral gains) cannot change arbitrary due to physical constraints of the system. For this aim, it is considered that the supplementary integral and proportional gains by ANN cannot exceed ± 0.4. Two scaling coefficients are also applied in the outputs of the ANN coordinator. The coefficients are optimized by using an SCA to provide an optimal ANN coordinator.

V. Case Study

A two-area power system is used to investigate the case studies. Each area contains three generating units, including reheat steam, hydro, and gas turbines, together with aggregated IACs. In each area, each type of generator is represented by a single equivalent model with its own unique inertia constant and speed regulation parameters. The details about their models and parameters are given in [1] and [30]. The base power of the system is 1000 MVA with a rated installed capacity of 2000 MW supplying 1760 MW of nominal load. The thermal power plants' output power is constrained by governor dead-bands with a GRC of 10% per minute (0.0017 p.u. MW/s) for dropping and rising rates. The hydro power units are restricted by GRCs of 360% per minute (0.06 p.u. MW/s) for dropping and 270% per minute (0.045 p.u. MW/s) for rising. Two IAC aggregators are supposed to be involved in the respective areas, each of which includes 30, 000 IACs. The parameters of the thermal and electrical model of IACs are given in Appendix. Fig. 4 illustrates the generalized LFC model for the IAC aggregator in the area i. A participation coefficient of 0.15 is considered for the IACs. The power limits of aggregators are set between $[-0.01, 0.01]$ p.u. The upper and lower limits of the dead zone for ACE_{IAC} are supposed to be ± 0.002 p.u. The proposed MPC design utilizes a prediction horizon and control horizon of 20 and 2, respectively, with a sampling interval of 0.1 seconds. The optimal weighting coefficients of the MPC are obtained as $Q_{MPC} = 0.8015$ and $R_{MPC} = 1.3622$.

The suggested LFC system is evaluated using the OPAL-RT real-time (RT) simulator. The power grid model created in MATLAB/SIMULINK is compiled with RT-LAB software to translate the model to C language for the RT simulation. To verify the presented scheme in real-time, the compiled model from the RT-LAB is loaded into the OPAL-RT. Fig. 5 shows the real-time experimental setup. A fixed-step solver with a sample time of 10 μs is used in RT-LAB configuration parameters. This entails running the test system model, the applied controllers, and the ANN coordinator.

A. Efficacy of the Proposed IAC Aggregation Control

To evaluate the proposed controller's dynamic performance, a 0.02 p.u. load increase is applied in area 1 and in area 2 at $t = 2$ s. Three different scenarios are investigated: A simple MPC, an MPC with feedback correction, and no support. Indeed, no support implies that the IAC aggregators will not participate in frequency regulation, meaning that system frequency will be maintained solely by the CGUs. The deviation in frequency and tie-line powers during the transient time is shown in Fig. 6. As can be seen, the MPC with feedback correction results in reduced frequency and tie-line power deviations compared to the simple MPC controller and to the scheme with no support. Fig. 7 depicts the regulatory capacity of the CGUs using the proposed controller. The figure illustrates that the CGUs adjust their output powers in response to load fluctuations. The power outputs of the two IAC aggregators with the MPCFC and MPC are compared in Fig. 8. As shown, the suggested controller allows the IAC aggregators to supply the system with greater power. In other words, the power amplitudes of IAC aggregators with MPCFC are slightly higher than those with the MPC controller. The output control signals of the MPC and MPCFC in both areas are shown in Fig. 9. To assess the proposed controller's robustness against uncertainties in system parameters, a sensitivity analysis is conducted. The uncertainties are included in the governor time constant of both steam and hydro turbines (T_s and T_h). The parameters have been adjusted, increasing from zero to 50 percent from their initial operational values. Fig. 10 shows the frequency deviation in both areas as the parameters vary. It indicates that dynamic responses are minimally influenced, leading to a consistent and robust performance despite variations in T_s and T_y.

B. Examination of Time Delay on Regulation Performance

In this subsection, the impact of aggregator response delay on the regulation performance is investigated. The aggregators

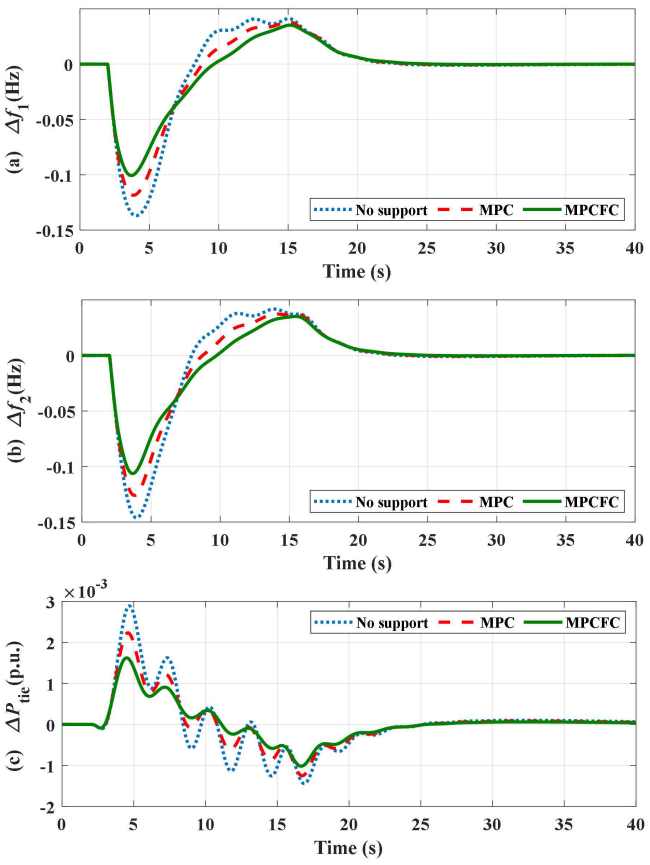

Fig. 6. Case A: frequency deviation of (a) area 1 (b) area 2; (c) tie-line power deviation.

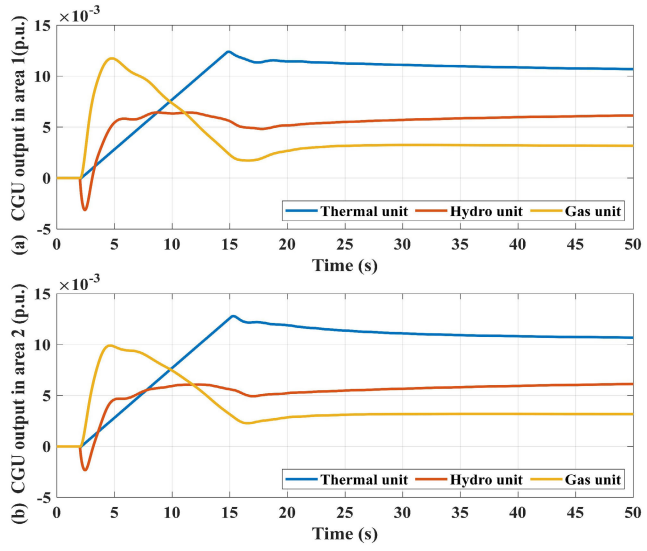

Fig. 7. Case A: power output of CGU units in (a) area 1 (b) area 2.

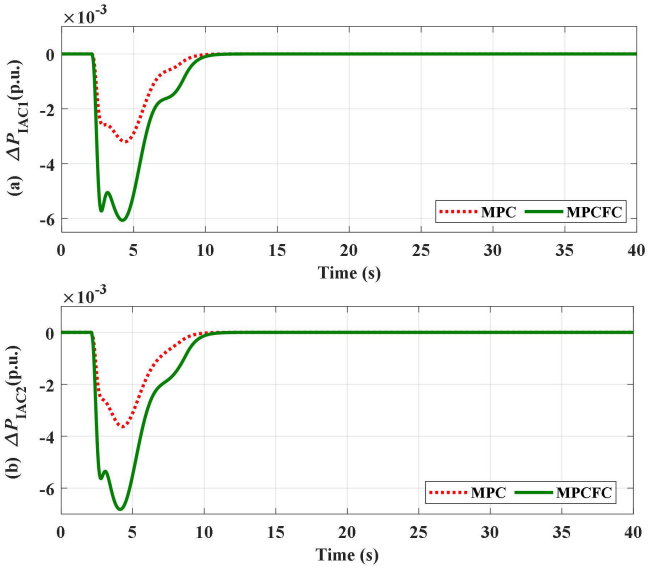

Fig. 8. Case A: power output of IAC aggregators in (a) area 1 (b) area 2.

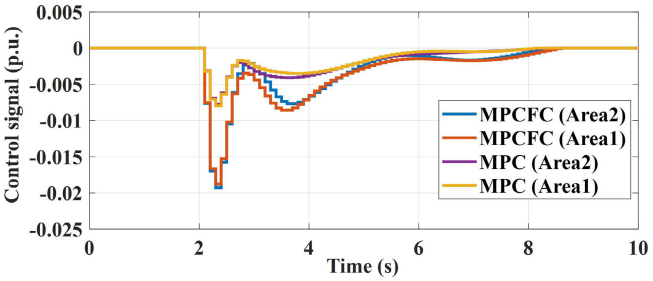

Fig. 9. Case A: output control signals of MPC and MPCFC.

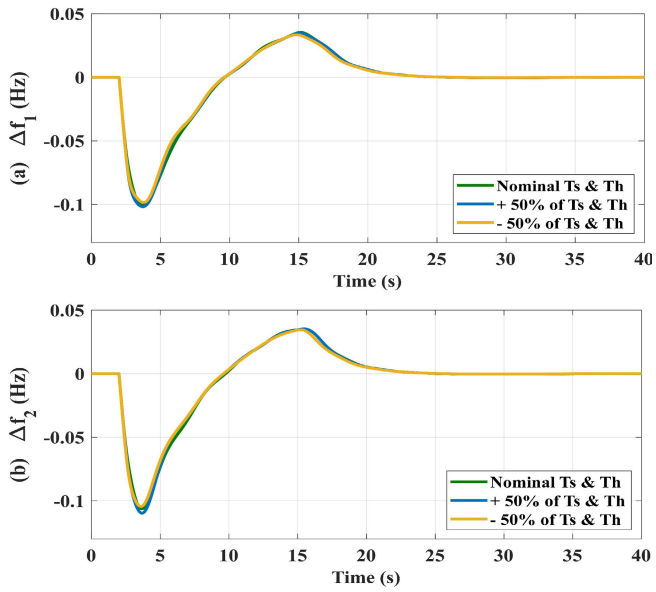

Fig. 10. Case A: frequency deviation of (a) area 1 (b) area 2 during ± 50% variations in T_s and T_h.

are assumed to receive the command signals with identical delays. The analysis is carried out for a step load increase of 0.02 p.u applied to load in area 1. The dynamic responses achieved by the MPCFC controller for various time delays are shown in Fig. 11. As can be seen, an increased time delay gives rise to increased frequency deviations and tie-line powers. This is due to the fact that the system lacks the power response of IACs due to the communication delay. Also, a delay-dependent robust stability criterion is employed to determine the maximum allowable time delay that ensures the LFC

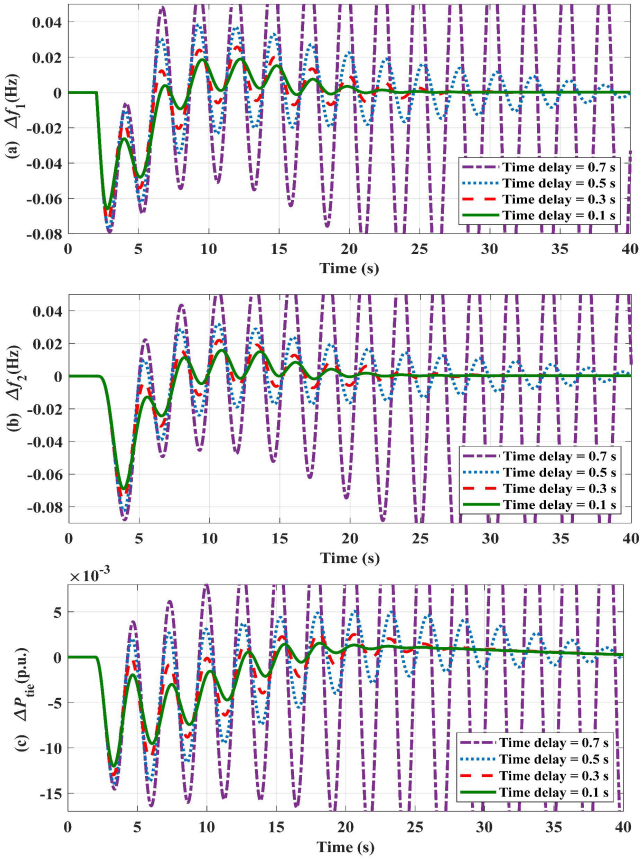

Fig. 11. Case B: frequency deviation of (a) area 1 (b) area 2; (c) tie-line power deviation.

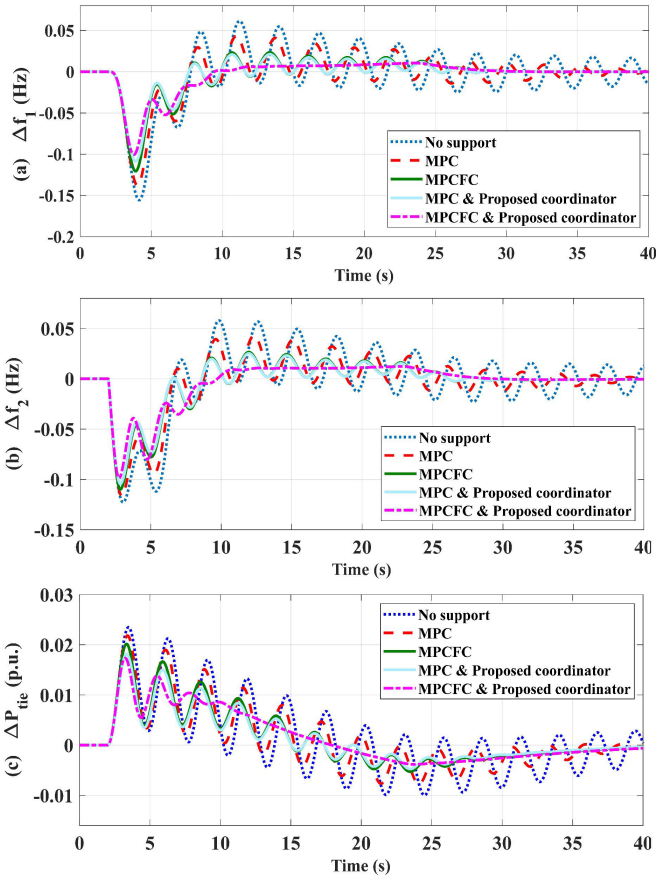

Fig. 12. Case C: frequency deviation of (a) area 1 (b) area 2; (c) tie-line power deviation.

system, integrated with the proposed control strategy, remains stable. The details about this stability criterion can be found in [31]. According to Theorem 1 given in [31], in Fig. 11, the allowable delay limit for system stability is determined to be 0.694 s for both IAC aggregators. In Fig.11, the frequency changes in both areas are presented for two specific time delays, both preceding and exceeding the delay boundary. Clearly, there is an instability in frequency fluctuation at 0.7 s, as this duration exceeds the established delay threshold.

C. Effectiveness of ANN Coordinator on Regulation Performance

An ANN coordinator is included in the closed-loop system to handle the significant frequency fluctuations brought on by transmission delays. The obtained scale coefficients for the ANN coordinator are obtained equal to 0.02 and 0.1 for the corresponding proportional and integral gains, respectively. The load in area 2 is expected to increase by 0.03p.u. at $t = 2$s. For the rest of the simulations, the communication delay is assumed to be 0.3 s. The frequency responses and tie-line power deviations are shown in Fig. 12 for the proposed MPCFC controller with the described ANN coordination, the proposed controller without a coordination scheme, and the MPC controller. The obtained results show that the proposed ANN-based coordinator scheme contributes efficiently to further reductions in the frequency and tie-line power overshoots compared to the schemes without coordination, thus resulting in superior performance, in particular in case of longer communication delays. Also, as observed, the MPC & proposed coordinator yields better frequency performance than the MPCFC without the proposed coordinator. This is primarily because the proposed coordinator provides the fine-tuning of the CGU units' secondary controller, which has a significant share in correcting generation and consumption mismatches in the system. However, it's worth noting that the MPCFC & proposed coordinator demonstrates superior frequency performance than the MPC & proposed coordinator.

D. Dynamic Response With Load Change and Wind Energy

With the same total number of IACs integrated into the grid, it is considered that a wind farm is connected to area 1. Fig. 13 shows a complex disturbance caused by the random output power of wind farm in conjunction with a load increase applied at $t = 25$ s to the load value in area 1. Under the described complex disturbance, the changes in frequencies and tie-line powers are plotted in Fig. 14 with a communication delay of 0.2 s. As can be seen, as with the other case studies, the dynamic responses exhibit lower oscillations with the MPCFC with the proposed supervisory control in comparison to the conventional MPC and to the scheme with no support. Additionally, the results demonstrate how well the suggested ANN-based coordination strategy

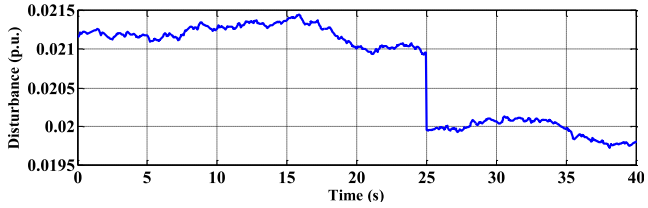

Fig. 13. Case D: Complex disturbances from load change and wind energy.

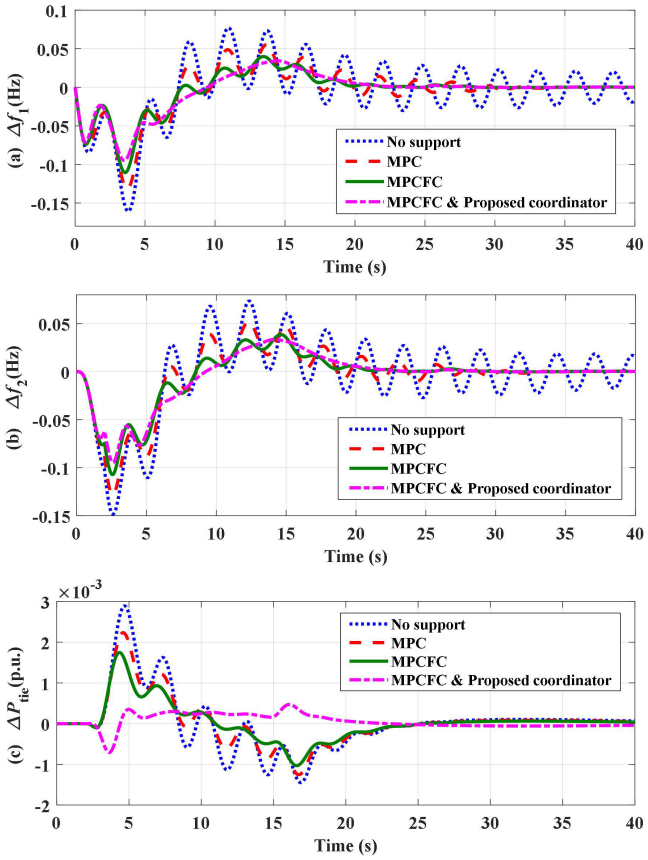

Fig. 14. Case D: frequency deviation of (a) area 1 (b) area 2; (c) tie-line power deviation.

works in reducing the frequency and tie-line power oscillations when there exist fluctuations in wind farm power and also time delay. The generated gains by the ANN coordinator are presented in Fig. 15 in response to the complex disturbance. The figure indicates that the ANN coordinator regulates the control parameters of CGUs in such a way that the least fluctuations are achieved in the frequency and tie-line powers.

E. Comparing With Model-Based Control Techniques

Here, a comparison study is conducted to investigate the performance of the proposed controller in a more critical situation. For this end, the controller's performance is compared to a linear quadratic regulator (LQR) and a fuzzy-PI controller. It's vital to note that the decision to choose these methods for comparison is established in their categorization as model-based control algorithms, similar to MPC and MPCFC. The uncertainty in the model is accounted for in the

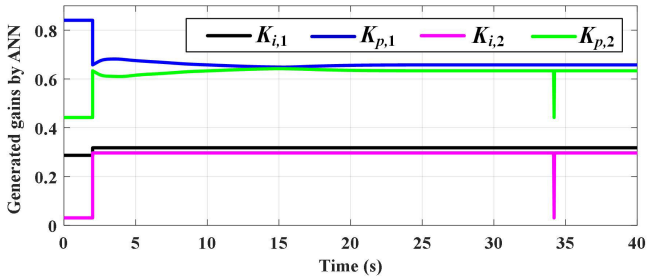

Fig. 15. Case D: The generated gains for CGUs controller by ANN.

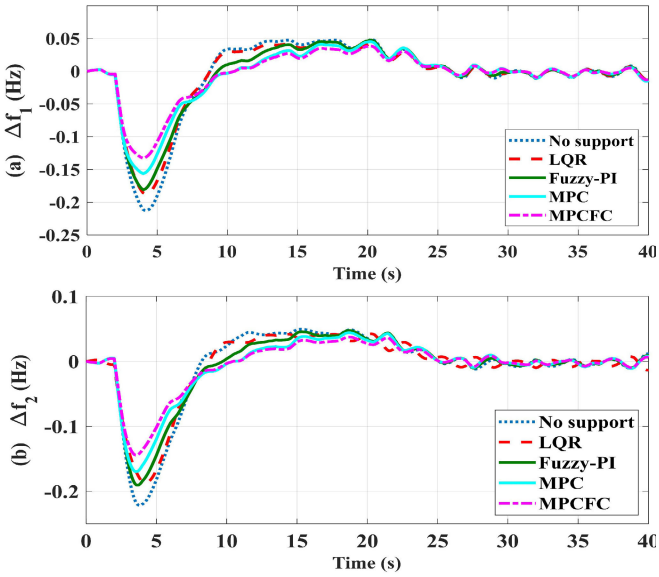

Fig. 16. Case E: Comparison between the proposed controller, MPC, LQR control, and fuzzy-PI control.

power flow across the tie-line between area 1 and area 2. This uncertainty is represented by a uniform disturbance, ranging between 2% above and below the actual value. A 0.03 p.u. load increase is applied in both areas. The frequency deviation in both areas is shown in Fig. 16. As observed, the proposed controller demonstrates better performance when compared to the conventional MPC, fuzzy-PI control, and LQR control. The efficiency of the fuzzy control is influenced by the fixed fuzzy rules applied during its design. In the case of LQR control, as a linear control approach, its performance and convergence rate are affected by the system's uncertainties.

VI. Conclusion

In this paper, a model predictive control (MPC) method is designed to control the inverter air conditioners (IACs) in load frequency control. A linear equivalent model of IACs is developed to be integrated into the proposed control structure. The MPC of IACs receives the ACE signal as the input and generates an appropriate signal for IACs to efficiently contribute to the LFC problem. The proposed MPC strategy consists of a feedback correction to improve the accuracy of the predictive ACE signal. To address the issue of time delay in the power grid model, an ANN supervisory coordinator is developed. The ANN generates supplementary gains for the

proportional-integral (PI) controller of the automatic generation control of conventional generation units. The contribution of the presented controller is analyzed in the LFC of a multi-area power system. The superior robustness properties of the presented MPC with feedback correction structure are indicated over other controlling approaches to handle various uncertainty sources like the load uncertainty and the uncertainty of wind turbine's power. The performance of the MPC with and without the ANN is assessed for different time delays. The time delay analysis indicates that the MPC without ANN coordinator is weak and even unable (when the time delay increases) to dampen the frequency and tie-line power deviations. However, the MPC with the proposed coordinator successfully maintains the performance throughout a broad range of time delays in the IAC aggregators' response. One direction for future research is to explore intelligent methods for real-time adjustment tuning of weighting factors in the MPCFC. This makes the control system more resilient and adaptable to various uncertainties arising from loading and operating conditions changes.

APPENDIX

TABLE I
THE PARAMETERS OF THE THERMAL AND ELECTRIC MODEL OF IACS

Parameter	Value	Unit	Parameter	Value	Unit
C_r	1.005	kJ/(kg.°C)	$f_{IAC}^{\min}$	150	Hz
V_r	250	m^3	c_{p1}	0.04	kW/Hz
ρ_d	1.205	kg/m^3	c_{p2}	0.02	kW
K_a	0.52	Hz/°C	c_{q1}	0.12	kW/Hz
K_b	0.032	Hz/(°C.s)	c_{q2}	-0.05	kW
$f_{IAC}^{\min}$	1	Hz	θ_{st}	25	°C

REFERENCES

[1] A. Oshnoei, M. Kheradmandi, R. Khezri, and A. Mahmoudi, "Robust model predictive control of gate-controlled series capacitor for LFC of power systems," *IEEE Trans. Ind. Informat.*, vol. 17, no. 7, pp. 4766–4776, Jul. 2021.

[2] X. Wang, D. Ding, X. Ge, and H. Dong, "Neural-network-based control with dynamic event-triggered mechanisms under DoS attacks and applications in load frequency control," *IEEE Trans. Circuits Syst. I, Reg. Papers*, vol. 69, no. 12, pp. 5312–5324, Dec. 2022, doi: 10.1109/TCSI.2022.3206370.

[3] Y. Arya, "Effect of electric vehicles on load frequency control in interconnected thermal and hydrothermal power systems utilising CF-FOIDF controller," *IET Gener., Transmiss. Distribution*, vol. 14, no. 14, pp. 2666–2675, May 2020.

[4] A. Oshnoei, M. Kheradmandi, F. Blaabjerg, N. D. Hatziargyriou, S. M. Muyeen, and A. Anvari-Moghaddam, "Coordinated control scheme for provision of frequency regulation service by virtual power plants," *Appl. Energy*, vol. 325, Nov. 2022, Art. no. 119734.

[5] M. R. Vedady Moghadam, R. T. B. Ma, and R. Zhang, "Distributed frequency control in smart grids via randomized demand response," *IEEE Trans. Smart Grid*, vol. 5, no. 6, pp. 2798–2809, Nov. 2014.

[6] K. Peddakapu, M. R. Mohamed, P. Srinivasarao, Y. Arya, P. K. Leung, and D. J. K. Kishore, "A state-of-the-art review on modern and future developments of AGC/LFC of conventional and renewable energy-based power systems," *Renew. Energy Focus*, vol. 43, pp. 146–171, Dec. 2022.

[7] A. Oshnoei, O. Sadeghian, and A. Anvari-Moghaddam, "Intelligent power control of inverter air conditioners in power systems: A brain emotional learning-based approach," *IEEE Trans. Power Syst.*, vol. 38, no. 5, pp. 4054–4068, Sep. 2023, doi: 10.1109/TPWRS.2022.3218589.

[8] H. Hui, Y. Ding, and M. Zheng, "Equivalent modeling of inverter air conditioners for providing frequency regulation service," *IEEE Trans. Ind. Electron.*, vol. 66, no. 2, pp. 1413–1423, Feb. 2019.

[9] X. Zhuang, C. Ye, Y. Ding, H. Hui, and B. Zou, "Data-driven reserve allocation with frequency security constraint considering inverter air conditioners," *IEEE Access*, vol. 7, pp. 120014–120022, 2019.

[10] B. Yildirim, M. Gheisarnejad, and M. H. Khooban, "Delay-dependent stability analysis of modern shipboard microgrids," *IEEE Trans. Circuits Syst. I, Reg. Papers*, vol. 68, no. 4, pp. 1693–1705, Apr. 2021, doi: 10.1109/TCSI.2021.3052774.

[11] L. Jin, Y. He, C.-K. Zhang, X.-C. Shangguan, L. Jiang, and M. Wu, "Robust delay-dependent load frequency control of wind power system based on a novel reconstructed model," *IEEE Trans. Cybern.*, vol. 52, no. 8, pp. 7825–7836, Aug. 2022.

[12] M. Song, C. Gao, J. Yang, and H. Yan, "Energy storage modeling of inverter air conditioning for output optimizing of wind generation in the electricity market," *CSEE J. Power Energy Syst.*, vol. 4, no. 3, pp. 305–315, Sep. 2018.

[13] X. Wu, J. He, Y. Xu, J. Lu, N. Lu, and X. Wang, "Hierarchical control of residential HVAC units for primary frequency regulation," *IEEE Trans. Smart Grid*, vol. 9, no. 4, pp. 3844–3856, Jul. 2018.

[14] W. Mendieta and C. A. Cañizares, "Primary frequency control in isolated microgrids using thermostatically controllable loads," *IEEE Trans. Smart Grid*, vol. 12, no. 1, pp. 93–105, Jan. 2021.

[15] T. Jiang, P. Ju, C. Wang, H. Li, and J. Liu, "Coordinated control of air-conditioning loads for system frequency regulation," *IEEE Trans. Smart Grid*, vol. 12, no. 1, pp. 548–560, Jan. 2021.

[16] H. Hui, Y. Ding, Z. Lin, P. Siano, and Y. Song, "Capacity allocation and optimal control of inverter air conditioners considering area control error in multi-area power systems," *IEEE Trans. Power Syst.*, vol. 35, no. 1, pp. 332–345, Jan. 2020.

[17] H. Hui, Y. Ding, T. Chen, S. Rahman, and Y. Song, "Dynamic and stability analysis of the power system with the control loop of inverter air conditioners," *IEEE Trans. Ind. Electron.*, vol. 68, no. 3, pp. 2725–2736, Mar. 2021, doi: 10.1109/TIE.2020.2975465.

[18] S. Oshnoei, M. R. Aghamohammadi, S. Oshnoei, S. Sahoo, A. Fathollahi, and M. H. Khooban, "A novel virtual inertia control strategy for frequency regulation of islanded microgrid using two-layer multiple model predictive control," *Appl. Energy*, vol. 343, Aug. 2023, Art. no. 121233.

[19] Z. Hu, S. Liu, W. Luo, and L. Wu, "Intrusion-detector-dependent distributed economic model predictive control for load frequency regulation with PEVs under cyber attacks," *IEEE Trans. Circuits Syst. I, Reg. Papers*, vol. 68, no. 9, pp. 3857–3868, Sep. 2021, doi: 10.1109/TCSI.2021.3089770.

[20] M. H. Khooban and M. Gheisarnejad, "Islanded microgrid frequency regulations concerning the integration of tidal power units: Real-time implementation," *IEEE Trans. Circuits Syst. II, Exp. Briefs*, vol. 67, no. 6, pp. 1099–1103, Jun. 2020, doi: 10.1109/TCSII.2019.2928838.

[21] N. Zhao et al., "Model predictive based frequency control of power system incorporating air-conditioning loads with communication delay," *Int. J. Electr. Power Energy Syst.*, vol. 138, Jun. 2022, Art. no. 107856.

[22] S. W. Ali et al., "Finite-control-set model predictive control for low-voltage-ride-through enhancement of PMSG based wind energy grid connection systems," *Mathematics*, vol. 10, no. 22, p. 4266, Nov. 2022.

[23] K. Shen, J. Feng, and J. Zhang, "Finite control set model predictive control with feedback correction for power converters," *CES Trans. Electr. Mach. Syst.*, vol. 2, no. 3, pp. 312–319, Sep. 2018.

[24] M. Elsisi, "Design of neural network predictive controller based on imperialist competitive algorithm for automatic voltage regulator," *Neural Comput. Appl.*, vol. 31, no. 9, pp. 5017–5027, Jan. 2019.

[25] P. Chen, L. Yu, and D. Zhang, "Event-triggered sliding mode control of power systems with communication delay and sensor faults," *IEEE Trans. Circuits Syst. I, Reg. Papers*, vol. 68, no. 2, pp. 797–807, Feb. 2021, doi: 10.1109/TCSI.2020.3035603.

[26] S. Oshnoei, A. Oshnoei, A. Mosallanejad, and F. Haghjoo, "Novel load frequency control scheme for an interconnected two-area power system including wind turbine generation and redox flow battery," *Int. J. Electr. Power Energy Syst.*, vol. 130, Sep. 2021, Art. no. 107033.

[27] S. A. Pourmousavi and M. H. Nehrir, "Introducing dynamic demand response in the LFC model," *IEEE Trans. Power Syst.*, vol. 29, no. 4, pp. 1562–1572, Jul. 2014.

[28] H. Sorouri, M. Sedighizadeh, A. Oshnoei, and R. Khezri, "An intelligent adaptive control of DC–DC power buck converters," *Int. J. Electr. Power Energy Syst.*, vol. 141, Oct. 2022, Art. no. 108099.

[29] J. Schmidhuber, "Deep learning in neural networks: An overview," *Neural Netw.*, vol. 61, pp. 85–117, Jan. 2015.
[30] A. Oshnoei, R. Khezri, and S. Muyeen, "Model predictive-based secondary frequency control considering heat pump water heaters," *Energies*, vol. 12, no. 3, p. 411, Jan. 2019.
[31] S. Oshnoei, A. Oshnoei, A. Mosallanejad, and F. Haghjoo, "Contribution of GCSC to regulate the frequency in multi-area power systems considering time delays: A new control outline based on fractional order controllers," *Int. J. Electr. Power Energy Syst.*, vol. 123, Dec. 2020, Art. no. 106197.

Arman Oshnoei (Member, IEEE) received the M.S. degree in electrical engineering from the University of Tabriz, Tabriz, Iran, in 2017, and the Ph.D. degree in electrical engineering from Shahid Beheshti University, Tehran, Iran, in 2021. From November 2020 to May 2021, he was a Visiting Ph.D. Scholar with the Department of Energy, Aalborg University, Aalborg, Denmark. From August 2021 to March 2022, he was a Research Assistant with Aalborg University. From May 2022 to October 2023, he was a Post-Doctoral Research Fellow with Aalborg University. He is currently an Assistant Professor of electrical power engineering with Aalborg University. His current research interests include the control and stability of power electronic-based power systems, energy storage systems, and intelligent control. He has been selected and awarded by the National Elite Foundation of Iran in 2019. He was a recipient of the Outstanding Researcher Award from Shahid Beheshti University in 2022.

Morteza Kheradmandi (Member, IEEE) received the B.S. and M.S. degrees in electrical engineering from the Sharif University of Technology, Tehran, Iran, in 1999 and 2001, respectively, and the Ph.D. degree from the Sharif University of Technology in collaboration with Institut National Polytechnique de Grenoble, Grenoble, France. His current research interests include power system dynamics, power system restoration, and power system operation and planning.

Rahmat Khezri (Senior Member, IEEE) received the M.S. degree in electrical engineering from the University of Kurdistan, Iran, and the Ph.D. degree in electrical engineering from Flinders University, Australia, in 2021. Over the past years, he was a Research Fellow and a Post-Doctoral Researcher with the University of Tsukuba, Japan; Aarhus University, Denmark; and the Chalmers University of Technology, Sweden. His current research interests include power system planning and operation, renewable energy, vehicle-to-grid, and battery energy storage systems.

Soroush Oshnoei (Associate Member, IEEE) received the B.Sc. degree in electrical engineering from the University of Tabriz, Tabriz, Iran, in 2016, and the M.Sc. degree in power systems from Shahid Beheshti University, Tehran, Iran, in 2018. Since 2022, he has been a Research Assistant with the Department of Electrical and Computer Engineering, Aarhus University, Aarhus, Denmark. His current research interests include cyber security of power systems and microgrids, the stability and control of power systems, and microgrids and intelligent control.

Amin Mahmoudi (Senior Member, IEEE) received the B.Sc. degree in electrical engineering from Shiraz University, Shiraz, Iran, in 2005, the M.Sc. degree in electrical power engineering from the Amirkabir University of Technology, Tehran, Iran, in 2008, and the Ph.D. degree from the University of Malaya, Kuala Lumpur, Malaysia, in 2013. He is currently a Senior Lecturer with Flinders University, Adelaide, Australia. He has authored/coauthored more than 170 papers in international journals and conferences. His current research interests include electrical energy conversion, electrical machines and drives, renewable energy systems, and hybrid power networks. It includes transportation electrification in which sustainable energy-efficient solutions are realized by advanced electric motors, power electronics, energy management systems and controls for electrified powertrains, and electric vehicles. He is a member of Engineers Australia (MIEAust) and a Chartered Professional Engineer (CPEng).

Maher A. Azzouz (Senior Member, IEEE) received the B.Sc. and M.Sc. degrees (Hons.) in electrical power engineering from Cairo University, Giza, Egypt, in 2008 and 2011, respectively, and the Ph.D. degree in electrical and computer engineering from the University of Waterloo, Waterloo, ON, Canada, in 2016. He was a Post-Doctoral Fellow with the Power and Energy System Group, University of Waterloo. He is currently on leave with the Department of Electrical and Computer Engineering, University of Windsor, Windsor, ON, Canada. He is with the Electrical Engineering Department, Qatar University, Qatar. His current research interests include the control of power electronic converters, power system protection, distribution system operation and planning, and renewable energy sources. He has been recognized as one of the best reviewers of IEEE TRANSACTIONS ON SMART GRID. He is a Registered Professional Engineer in the Province of Ontario.

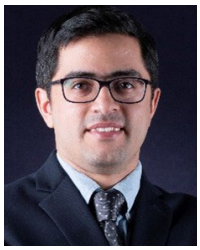

Ahmed S. A. Awad (Senior Member, IEEE) received the B.Sc. and M.Sc. degrees in electrical engineering from Ain Shams University, Cairo, Egypt, in 2007 and 2010, respectively, and the Ph.D. degree from the Electrical and Computer Engineering Department, University of Waterloo, Waterloo, ON, Canada, in 2014. He is currently an Assistant Professor with the Electrical and Computer Engineering Department, Sultan Qaboos University, Muscat, Oman, and an Adjunct Associate Professor with the Electrical and Computer Engineering Department, University of Windsor, ON, Canada. His current research interests include the integration of sustainable energy technologies into power systems, electricity market equilibrium, and the operation and control of power systems. He is currently an Editor of IEEE TRANSACTIONS ON SUSTAINABLE ENERGY and a Registered Professional Engineer in the Province of Ontario, Canada.